Entrapment of ball-milled biochar in Ca-alginate beads for the removal of aqueous Cd(II)

Bing Wang[a,b], Bin Gao[b,*], Yongshan Wan[c]

[a] State Key Laboratory of Environmental Geochemistry, Institute of Geochemistry, Chinese Academy of Sciences, Guiyang 550081, China
[b] Department of Agricultural and Biological Engineering, University of Florida, Gainesville, FL 32611, USA
[c] National Health and Environmental Effects Research Laboratory, US EPA, Gulf Breeze, FL 32561, USA

ABSTRACT

A novel adsorbent was synthesized through the entrapment of ball-milled biochar in Ca-alginate beads for the removal of aqueous Cd(II). Batch adsorption experiments were conducted to compare Cd(II) adsorption characteristics of ball-milled biochar (BMB), Ca-alginate (CA), and Ca-alginate entrapped ball-milled biochar (CA-BMB). All the tested adsorbents showed excellent sorption ability. The maximum Cd (II) adsorption capacity estimated with Langmuir isotherm modeling was 251.8 mg g^{-1} for CA, 227.1 mg g^{-1} for CA-BMB, and 40.0 mg g^{-1} for BMB. The results demonstrate that entrapment of ball-milled biochar in Ca-alginate provides a low-cost and high-effective way for the removal of aqueous Cd (II).

© 2017 The Korean Society of Industrial and Engineering Chemistry. Published by Elsevier B.V. All rights reserved.

Introduction

Heavy metal pollution remains a worldwide issue affecting human health and the environment. Cadmium (Cd), classified as a human carcinogen, is extremely toxic, with permissible exposure limits much lower than other heavy metals. The US EPA has established a Maximum Contaminant Level of 0.005 mg/L for cadmium in drinking water while the World Health Organization established a guideline of 0.003 mg/L for lifetime consumption. As a naturally occurring element, Cd exists in earth crust at only about 0.1 mg/kg; yet anthropogenic sources of Cd, mostly released during the manufacture of numerous industrial products or as a byproduct of zinc production, pose special challenges for pollution control [1]. Cadmium is highly soluble in water as a divalent cation, Cd(II). Since it is not biodegradable in the environment, Cd(II) may be transported in one setting to another, and eventually become enriched through bio-accumulation in the ecosystem. Ingestion of water and food containing elevated levels of Cd(II) (e.g., crustaceans, mullosks, and organ meats) is a major route of Cd (II) exposure, which can result in long-term health effects such as damages to the liver and kidneys and cardiovascular diseases [2,3].

Research and development of low-cost and efficient technology to remove cadmium from wastewater continue to draw interests in the science and engineering community [4]. A significant amount of research has been conducted on adsorption technology to remove cadmium ions from aqueous solutions [5]. Activated carbon, as the most commonly used adsorbent, has a good adsorption effect; yet its use on a large scale is limited by the difficulties involved in process engineering such as the dispersion of activated carbon powder and high cost for recovery [6]. In recent years, biochar has been studied as a low-cost adsorbent, which may offer great benefits in environmental and agricultural applications because of its large surface area, porous structure, and abundant functional groups [7–14]. In particular, several researchers have developed various novel engineering methods to functionalize raw biochar to expand its environmental applications for either removing targeted pollutants or enhancing its adsorption capacities [15–24].

Ball milling is a new method that has been introduced into the biochar research field to improve its adsorption capacity [25,26]. The principle is that the biochar can be ground through the ball to nano-sized particles, thereby enhancing the specific surface area of the material, which, in turn, increases its adsorption capacity [27,28]. However, the ball-milled biochar is usually very tiny particles and can easily spread in water [29,30]. This may result in secondary damages to the environment and human health [31,32]. In this study, ball-milled biochar was entrapped and stabilized in

calcium alginate to make it more stable and environmentally friendly. In addition, it is anticipated that the distribution of the ball-milled biochar in the composite would improve its sorption performance. Alginate is an anionic polysaccharide in the outer cell wall of brown algae. The major component of alginate is alginic acid, which is a polymer with abundant free hydroxyl and carboxyl groups distributed along the polymer chain backbone. The uptake of metal ions in solution is mostly through ion exchange between protons of the free carboxylic functional groups of the alginate and the metal ions from the solutions. The commercial alginate, sodium alginate, has been widely used in biomedical science and engineering for its favorable properties such as biocompatibility and ease of gelation [33]. Sodium alginate, when dissolved in water, forms a viscous solution which possesses gel properties in spite of its weak gel strength. The gel is soft and soluble in alkaline solution. When Ca^{2+} is added to the solution, Ca^{2+} displaces part of H^+ and Na^+ to form calcium alginate (CA) gel. Recently, biochar impregnated with calcium alginate has been applied in wastewater treatment for removal of phosphate and selected heavy metals [34–36]. This study is the first one to report the effectiveness of ball-milled biochar impregnated with Ca-alginate as an adsorbent to remove Cd(II) in aqueous solutions.

The objectives of this study were to evaluate and compare the adsorption of Cd(II) on ball-milled biochar (BMB), calcium alginate (CA), and ball-milled biochar impregnated with calcium alginate (CA-BMB). It was hypothesized that the adsorption capacity of BMB to Cd(II) would be improved when impregnated with Ca-alginate. Specifically, the effects of pH and adsorbent dosage on Cd(II) adsorption as well as the adsorption kinetics and isotherms were examined through a series of batch adsorption experiments. The ultimate aim of this work was to develop a novel adsorbent derived from ball-milled biochar impregnated with Ca-alginate to remove cadmium ions from aqueous solutions.

Experimental

Chemicals and reagents

Reagent grade chemicals including cadmium nitrate tetrahydrate ($Cd(NO_3)_2 \cdot 4H_2O$) (ACROS Organics), calcium chloride ($CaCl_2$), sodium hydroxide (NaOH), nitric acid (HNO_3), sodium alginate was purchased from Fisher Scientific and used without further purification. Stock solutions of Cd(II) ($1000\,mg\,L^{-1}$) were prepared by dissolving $Cd(NO_3)_2 \cdot 4H_2O$ (Acros) volumetrically in deionized water. All glassware and PE centrifuge tubes were acid washed in a hydrochloric acid bath (10% HCl) and rinsed with deionized water.

Preparation of the ball-milled biochar and beads

Biochar used in this study originated from the bamboo feedstock. The raw materials were oven dried (80 °C) and converted into biochar through slow pyrolysis using a furnace (Olympic 1823HE) in a N_2 environment at temperatures of 450 °C. The biochar was mechanically activated in a planetary ball mill (Across International, PQ-N$_2$) at room temperature using 500 mL capacity agate milling jars and lids. The milling media consisted of an agate vial with $5 \times 20\,mm$ and $10 \times 10\,mm$ agate balls. In all milling runs the ball-to-powder weight ratio was 10:1 and the rotational speed of the main disk was 500 rpm. In each run, the biochar was milled for a total of 12 h (four 3-h rotations in alternative directions with a 10-min rest period in between). After milling, samples were collected and saved for use.

In order to get a uniform dispersion of sodium alginate-BMB aqueous solution, Na-alginate from macrosytica pyrifera, high viscosity (MP Biomedicals, Inc. Co., USA) was used. The ball-milled biochar (BMB) was added into a liquid state of sodium alginate

(1% w/v) at the mass ratio of 1:0.25 (BMB/alginate). An ultrasound was applied to disperse BMB in the solution for 30 h at 25 °C using a B3510-MT Ultrasonic Cleaner with a nominal frequency of 40 kHz (Branson Ultrasonics Co., USA). An aliquot of 100 mL sodium alginate-BMB mixture was then added dropwise into 500 mL 0.1 M $CaCl_2$ solution using a 60-mL syringe fitted with 23G1 Precision Glide needles to form Ca-alginate-BMB beads. Ca-alginate-BMB beads were left overnight to stabilize. The beads were washed with deionized water for several times to remove residual BMB particles and non- impregnated calcium ions. To compare the adsorption performance between non-immobilized and BMB-immobilized beads, pure Ca-alginate beads were prepared separately as a control. Similarly, the sodium alginate solution (same concentration as for the CA-BMB beads preparation) was added dropwise into 0.1 M $CaCl_2$ solution under magnetic stirring condition to obtain a homogeneous colloidal suspension to form the CA beads. Similarly, the beads were left overnight and washed with deionized water. Pre-experiments showed that the as-prepared beads were very stable in aqueous solution under various solution ionic strength and pH conditions. The diameters of non-dried and dried beads were about $2.30 \pm 0.04\,mm$ and $0.50 \pm 0.02\,mm$, respectively.

Characterizations of adsorbents

The structure and surface morphology of bamboo biochar (BB), ball-milled biochar (BMB), Ca-alginate (CA) and CA-BMB were characterized by scanning electron microscopy (SEM) (JSM-6400 Scanning Microscope, JEOL, Tokyo, Japan). The specific surface area and pore size distributions of the sorbents were measured by N_2 sorptometry on a Quantachrome Autosorb I, at 77 K. Samples were degassed under vacuum for least 24 h at 180 °C prior to analysis. Surface area was calculated according to the BET theory using adsorption data in the 0.01–0.3 relative pressure range. Pore volumes were calculated using Barrett-Joyner-Halenda (BJH) theory using desorption leg data.

Cd adsorption

Four batch adsorption experiments were conducted with CA, BMB and CA-BMB: pH effect experiment, dosage effect experiment, kinetics experiment, and isotherm experiment. The effect of pH on Cd(II) adsorption was investigated with initial pH of $50\,mg\,L^{-1}$ Cd (II) solutions adjusted to 2, 3, 4, 5, 6, 7, and 8 using 0.1 M HNO_3 or 0.1 M NaOH. The batch adsorption was initiated by mixing 0.010 g of each adsorbent with 40 mL of Cd(II) solutions in 50 mL Centrifuge Tubes (Fisher Scientific). The tubes were shaken on a New Brunswick rotary shaker at 150 rpm and 25 °C for 24 h. After shaking, samples were filtered using a 0.22 μm syringe filter (PVDF syringe filter; Whatman). The concentration of Cd(II) in solutions was measured immediately after filtration with an Inductively Coupled Plasma Optical Emission Spectrometer (ICP-OES), Optima 2100 DV, Perkin Elmer, USA. Calibration standards for Cd(II) were prepared at 5 levels including 0, 1.0, 2.0, 5.0 and $10.0\,mg\,L^{-1}$. Based on the result of the pH effect experiment, all subsequent sorption experiments in this study were conducted at pH = 5.0.

The dosage experiment was conducted with adsorbent of 0.0010 g, 0.0025 g, 0.0050 g, 0.0100 g, 0.0150 g, 0.0200 g, 0.0250 g and 0.0300 g added into 40 mL $50\,mg\,L^{-1}$ Cd(II) solution, respectively, and shaken on the mechanical shaker for 24 h. Sorption kinetics of Cd(II) were examined by mixing 0.010 g of the sorbent with 40 mL of $50\,mg\,L^{-1}$ Cd(II) solutions shaken on the mechanical shaker at time interval of 0.083, 0.5, 1, 2, 4, 8, 16 and 24 h. Sorption isotherms were conducted by mixing 0.010 g of each adsorbent with 40 mL of Cd(II) solution of varying concentrations ($5–300\,mg\,L^{-1}$) shaken on the mechanical shaker for 24 h. All

samples were immediately filtered after shaking and Cd concentrations in the solution determined as in the pH effect experiment.

All the adsorption experiments were conducted in triplicate at 25 °C, and the average experimental data were reported. The quantity of Cd(II) adsorbed onto adsorbents was calculated with Cd(II) concentrations in the initial and final solutions. Kinetic and isotherm models were developed using non-linear regression. Differences between the means were statistically analyzed with one-way ANOVA followed by Fisher's Least Significant Difference test at a significance level of $\alpha = 0.05$.

Results and discussion

Characterization of materials

The BMB used in this study had a surface area of 298.6 m^2 g^{-1}, about 16 times higher than the original bamboo biochar (18.2 m^2 g^{-1}), indicating that ball milling significantly increased the surface area of the biochar [25,26,28]. The surface area instrument was able to provide reliable measurements of the dried CA and CA-BMB beads, probably because the pore structures of the bead collapsed after drying. The SEM image of bamboo biochar (BB) exhibited smooth surface of the material with trace particles at nano-size (Fig. 1). In contrast, the ball-milled biochar (BMB) contained many of the nano-sized particles, confirming the CA-

based composite helped the distribution and stabilization of BMB particles. The CA and CA-BMB beads were both at sand-size; yet the surface of CA-BMB was much rougher than that of CA, reflecting the effect of the nano-sized BMB entrapped in CA.

Effect of pH

Adsorption of Cd(II), in general, increased with increasing pH in the pH range of 2–8 (Fig. 2) [32,33]. However, the increase reached a maximum at pH = 5 for CA and at pH = 4–7 for CA-BMB. Further increase in pH resulted in slight declines in Cd(II) adsorption. Changes in Cd(II) adsorption with pH manifested the effects of hydrogen ion concentrations on speciation of heavy metal ions and distribution of charge on the surface of the adsorbent material [34,37]. Previous studies have shown that the ball-milled bamboo biochar has abundant oxygen-containing functional groups, particularly carboxyl groups on its surface [26]. The acid functional groups along the molecule chain of alginate and in the surface of biochar could be changed by protonation and deprotonation of carboxyl groups. Thus, at lower pH (<4), Cd(II) adsorption is low due to the competition for adsorption sites between hydrogen and metal ions [39]. At high pH (>7), the formation of hydroxide anionic complexes could reduce the degree of freedom of metal ions. Therefore, too high or too low pH value is not conducive to adsorption of Cd(II). Previous studies have shown that pH of
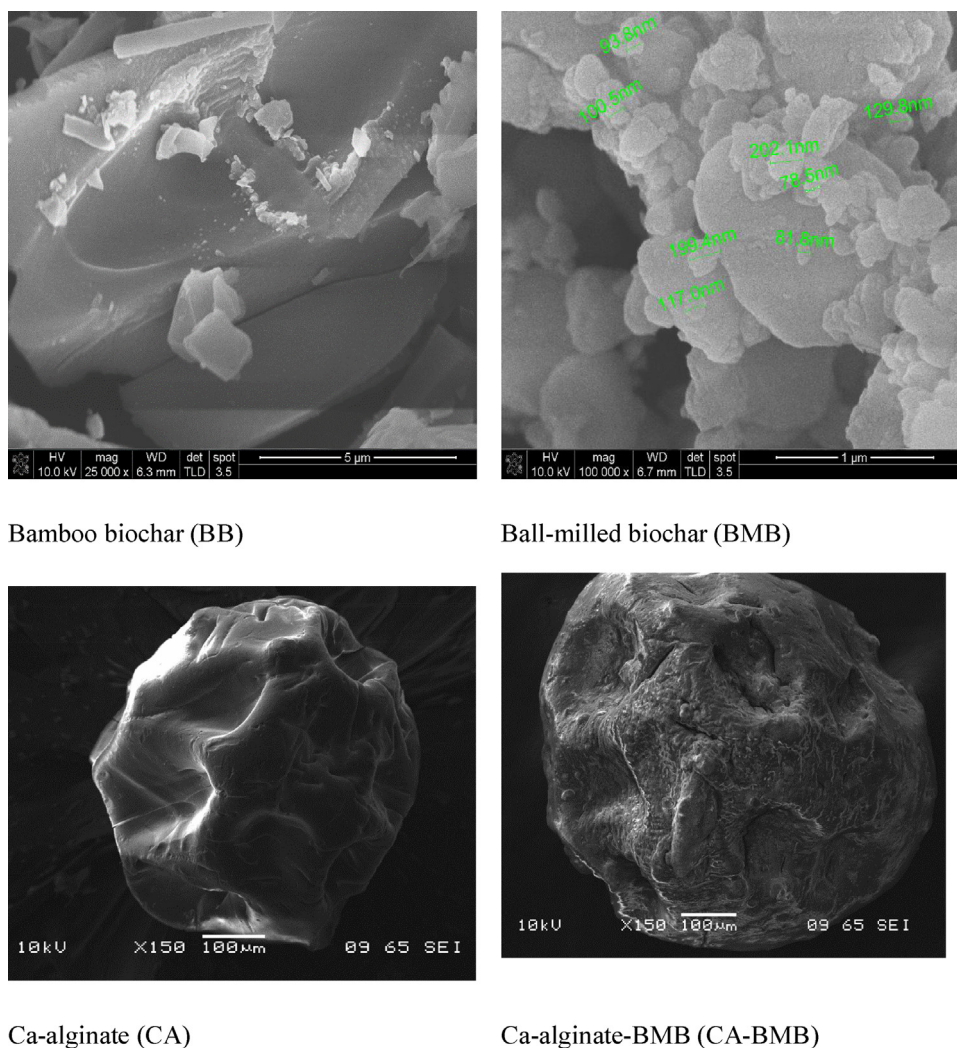

Bamboo biochar (BB)

Ball-milled biochar (BMB)

Ca-alginate (CA)

Ca-alginate-BMB (CA-BMB)

Fig. 1. Scanning electron microscope (SEM) images of BB, BMB, CA and CA-BMB.
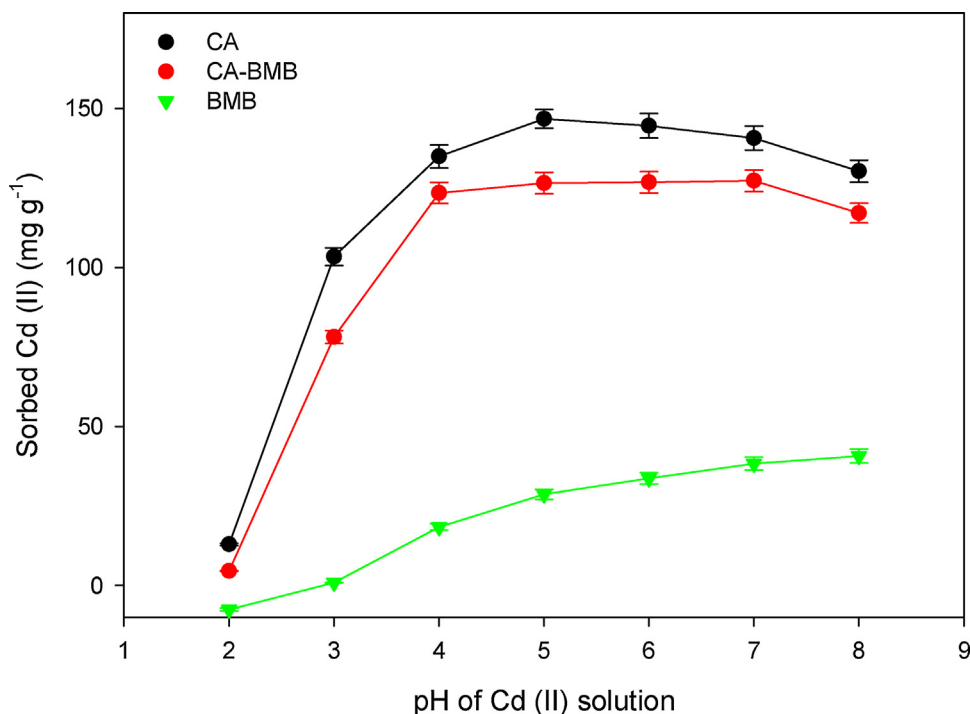
Fig. 2. Adsorption capacity of Cd(II) at different pH (initial Cd(II) concentration of 50 mg L^{-1}, contact time 24 h, temperature 25 °C, adsorbent dose 250 mg L^{-1}, and Cd(II) solution 40 mL) by CA, BMB, and CA-BMB. Error bars represent standard error of triplicate samples (n = 3). Symbols may cover error bars.

5.0–6.0 was optimum for Cd(II) adsorption [37,38], and this study, in general, supports this observation. This is also consistent with Papageorgious and Kouvelos [39] who reported that the pK$_a$ value of carboxylic groups in the alginate ranged from 3.4 to 3.9, meaning that alginate would become positively charged if pH was below these values. Thus, all subsequent sorption experiments in this study were conducted at pH 5.0.

Effect of adsorbent dosage

The Cd(II) removal rate increased sharply with increasing dosage from 1 mg to 10 mg [37], and the increase in Cd(II) removal rate slowed down with further increase in dosage (Fig. 3). The decrease in adsorbed Cd(II) at large adsorbent dose is possibly due to unsaturation of adsorption sites. In other words, the adsorbent
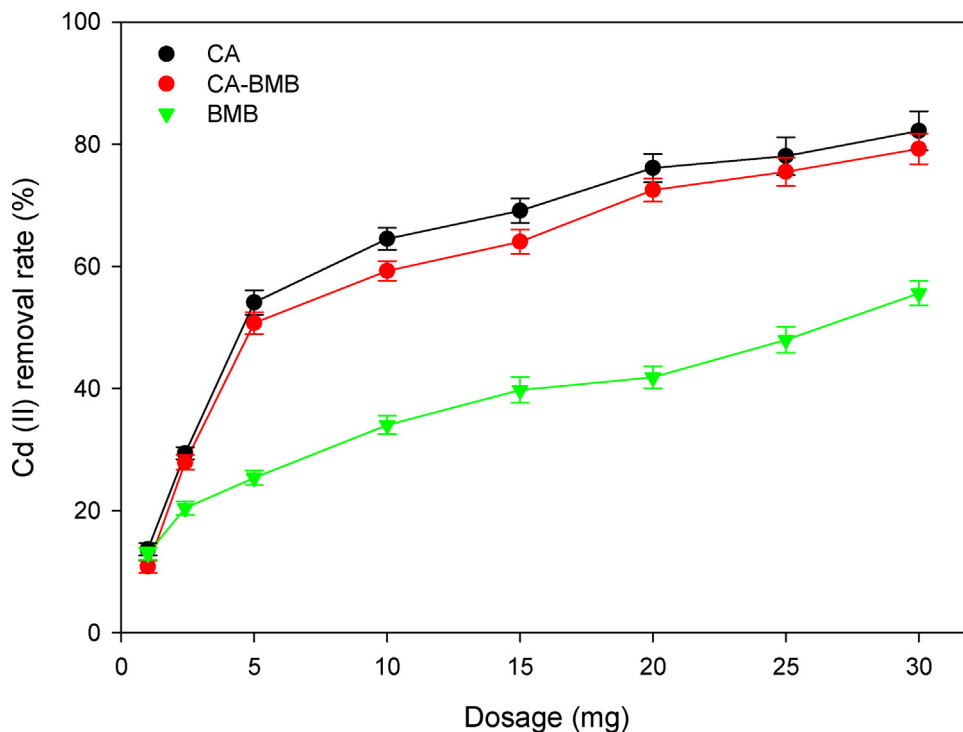

Fig. 3. Effect of CA-BMB dosage on Cd(II) removal (initial Cd(II) concentration 50 mg L^{-1}, contact time 24 h, temperature 25 °C, Cd(II) solution 40 mL, and pH 5.0). Error bars represent standard error of triplicate samples (n = 3). Symbols may cover error bars.
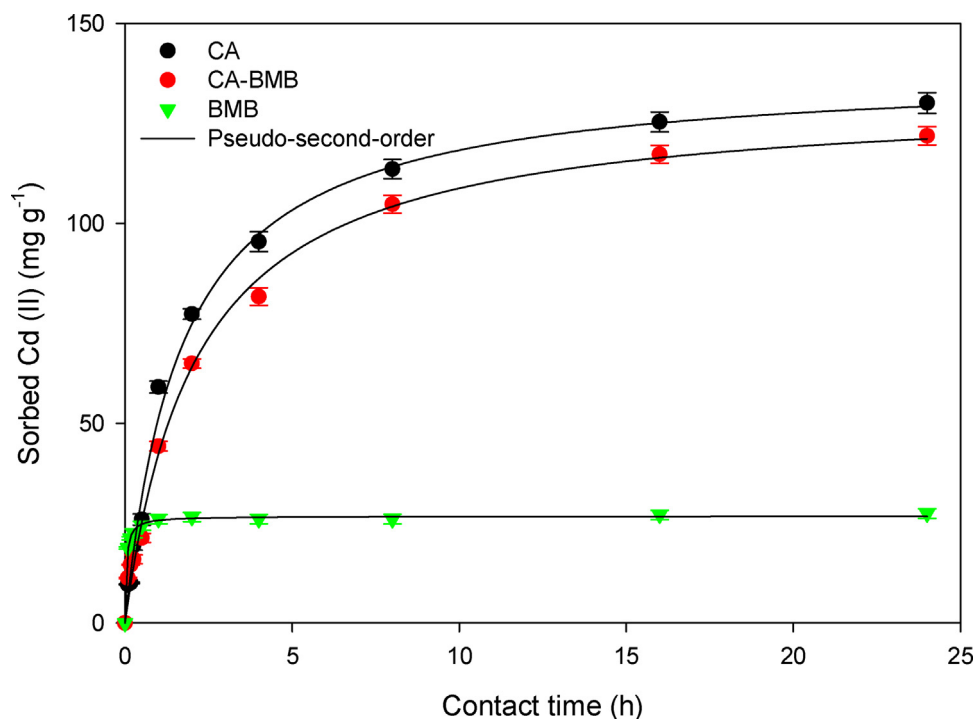
Fig. 4. The effect of contact time on the removal of Cd(II) by CA, BMB and CA-BMB (initial Cd(II) concentration 50 mg L^{-1}, temperature 25 °C, adsorbent dose 250 mg L^{-1}, Cd(II) solution 40 mL, and pH 5.0). The solid line is a pseudo-second-order kinetic model. Error bars represent standard error of triplicate samples (n = 3). Symbols may cover error bars.

was not efficiently used for removal of Cd(II) at large dosage rates. Another cause may be associated with aggregation between particles at high adsorbent concentrations, thereby reducing the total surface area of the adsorbent. Hence, the optimal dosage for removal of Cd(II) was found to be 250 mg L^{-1} for initial Cd(II) concentration 50 mg L^{-1} or 0.010 g in 40 mL Cd(II) solution.

Adsorption kinetics

Fig. 4 shows the adsorption kinetics of Cd(II) on CA, BMB and CA-BMB in solutions of 50 mg L^{-1}. The uptake process of Cd(II) for BMB was relatively fast with 95% of the adsorption completed in about 1 h. However, the adsorption of Cd(II) by CA and CA-BMB exhibited an initial rapid uptake with about 81.7% and 86.0% of Cd(II) adsorption completed within 8 h followed by slow kinetics that reached a plateau. This result suggests that Cd(II) diffusion in the pore networks of the CA-based beads might play an important role in controlling the adsorption kinetics of two adsorbents. The Cd(II) adsorption by CA and CA-BMB was 109.6 mg g^{-1} and 104.8 mg g^{-1}, respectively, which corresponded to 59.0% and 56.5% removal efficiency. At 16 h, the Cd(II) removal efficiency increased only to 68% and 67%, which were not significantly different from that for equilibration at 24 h (P < 0.05).

In general, the adsorption process can be divided into three successive stages: the first stage is called the external diffusion of the particles, and the adsorbate diffuses from the solution to the surface of the adsorbent. The second stage is called the pore diffusion, whereby the adsorbate continues to diffuse into the adsorbent pores in the adsorbent pores; The third stage is called the adsorption reaction stage, and the adsorbate is adsorbed on the surface within the pores of the adsorbent [39]. Identification of these three stages are not always directly obvious in the kinetics plot (e.g., Fig. 4); yet the data generally support two stage processes in which the initial fast adsorption is driven by external mass transfer to active sites while the later slow adsorption stage

indicates that the high-affinity binding sites are occupied, and the residual binding sites are gradually filled [37].

Sorption kinetic modeling of the experimental data helps understand the potential mechanisms in the sorption process [39]. In order to compare the adsorptive rate of different sorbents, pseudo-first-order, pseudo-second-order, Elovich and Ritchie models were used to simulate the sorption kinetic data:

$$q_t = q_e\left(1 - e^{-k_1 t}\right), \text{Pseudo} - \text{first} - \text{order} \qquad (1)$$

$$q_t = \frac{k_2 q_e^2 t}{1 + k_2 q_e t}, \text{Pseudo} - \text{second} - \text{order} \qquad (2)$$

$$q_t = \frac{1}{\beta}\ln(\alpha\beta t + 1), \text{Elovich} \qquad (3)$$

$$q_t = q_e - \left(q_e^{1-n}\frac{k_n}{1-n}t\right)^{\frac{1}{1-n}}, \text{Ritchie} \qquad (4)$$

where q_t (mg g^{-1}) and q_e (mg g^{-1}) are the adsorbed amounts of Cd(II) at time t and at equilibrium, respectively; k_1 (h^{-1}), k_2 (g mg^{-1} h^{-1}), and k_n (g^{n-1} mg^{1-n} h^{-1}) are the first-order, second-order, and Ritchie nth-order sorption rate constants. α (mg g^{-1} h^{-1}) is the initial sorption rate, and β (g mg^{-1}) is the desorption constant. The corresponding fitting parameters are listed in Table 1.

Usually, pseudo-first-order kinetics are applied to the process of pure physical adsorption. The pseudo-second-order kinetics assumes that the rate-limiting step is chemical adsorption or physicochemical adsorption. The adsorption process involves the transfer, exchange, and co-occurrence of electrons. As shown in Fig. 4, Cd(II) adsorption reached equilibrium in 24 h. According to the fit to different adsorption kinetics models (Table 1), the

Table 1

Summary best-fit parameters of various kinetic models for Cd(II) adsorption onto CA, BMB and CA-BMB.

Adsorbent	Model	Parameter 1	Parameter 2	R^2
CA	Pseudo-first-order	$k_1 = 0.510$	$q_e = 122.0$	0.982
	Pseudo-second-order	$k_2 = 0.00448$	$q_e = 137.8$	0.995
	Elovich	$\alpha = 148.4$	$\beta = 0.0347$	0.978
	Ritchie	$k_n = 0.00325$	$q_e = 140.0$	0.995
BMB	Pseudo-first-order	$k_1 = 12.6$	$q_e = 25.9$	0.971
	Pseudo-second-order	$k_2 = 0.944$	$q_e = 26.7$	0.996
	Elovich	$\alpha = 9134$	$\beta = 0.38$	0.809
	Ritchie	$k_n = 0.601$	$q_e = 27.2$	0.997
CA-BMB	Pseudo-first-order	$k_1 = 0.390$	$q_e = 115.6$	0.983
	Pseudo-second-order	$k_2 = 0.00358$	$q_e = 131.9$	0.995
	Elovich	$\alpha = 107.1$	$\beta = 0.0351$	0.990
	Ritchie	$k_n = 0.0000141$	$q_e = 115.5$	0.983

Table 2

Summary best-fit isotherm model parameters for sorption of Cd(II) onto the studied sorbents.

Adsorbent	Langmuir adsorption model			Freundlich adsorption model		
	Q_o (mg g^{-1})	k_L	R^2	k_f	$1/n$	R^2
Ca-alginate	251.8	0.058	0.989	48.7	3.29	0.964
BMB	40.0	0.198	0.984	14.7	5.23	0.944
Ca-alginate-BMB	227.1	0.052	0.985	43.0	3.29	0.970

pseudo-second-order model seems to be the best model describing the kinetics experimental data. Thus, the Cd(II) adsorption process by CA, BMB and CA-BMB was largely controlled by chemical adsorption. The relative magnitude of the adsorptive rate represented by constant K_2 in Table 2 indicated that the BMB reached equilibrium earlier than CA and CA-BMB.

Adsorption isotherms

Equilibrium Cd(II) adsorption isotherms of CA, BMB and CA-BMB were generated using a dosage of 0.010 g dry weight in 40 mL solution with a 24 h contact time (Fig. 5). Equilibrium sorption isotherm modeling was used to better understand the mechanism of adsorption and to identify the maximum sorption capacity of each material. According to Gibbs adsorption isothermal classification, Cd(II) adsorption isotherm belongs to L2 type, so Langmuir and Freundlich models were used to simulate the data. The hypothesis of the Langmuir model theory is that a monolayer is adsorbed on the homogeneous surface and that there is no interaction between the adsorbed molecules. The Freundlich model describes multilayer adsorption, whereby adsorption capacity continues to increase with increasing equilibrium concentrations. The Langmuir adsorption model and Freundlich adsorption model are expressed in the following equations:

Langmuir isotherm: $q_e = Q_o \cdot k_L \cdot C_e / (1 + k_L \cdot C_e)$ \hfill (5)

Freundlich isotherm: $q_e = k_f \cdot C_e^{1/n}$ \hfill (6)

where q_e (mg g^{-1}) is the adsorption capacity; C_e (mg L^{-1}) is the equilibrium concentration after the adsorption or desorption; $1/n$ (dimensionless) is the adsorption affinity; k_f (mg$^{1-1/n}$ L$^{1/n}$ g^{-1}) is the Freundlich adsorption constant; Q_o (mg g^{-1}) is the maximum sorption capacity; k_L (L mg^{-1}) is the Langmuir constant.

For all three sorbents, the Langmuir equation better simulated the data than the Freundlich equation (i.e., higher R^2 in Table 2). This suggests that these materials interacted with Cd(II) as a homogenous surface along with monolayer adsorption. Because both CA and BMB were rich in surface functional group, it was suspected that Cd(II) adsorption onto the three adsorbents (i.e., BMB, CA, and CA-BMB) was mainly controlled via the interactions between the metal contaminant and the acidic oxygen-containing functional groups [9]. According to the fitting isotherms (Table 2),
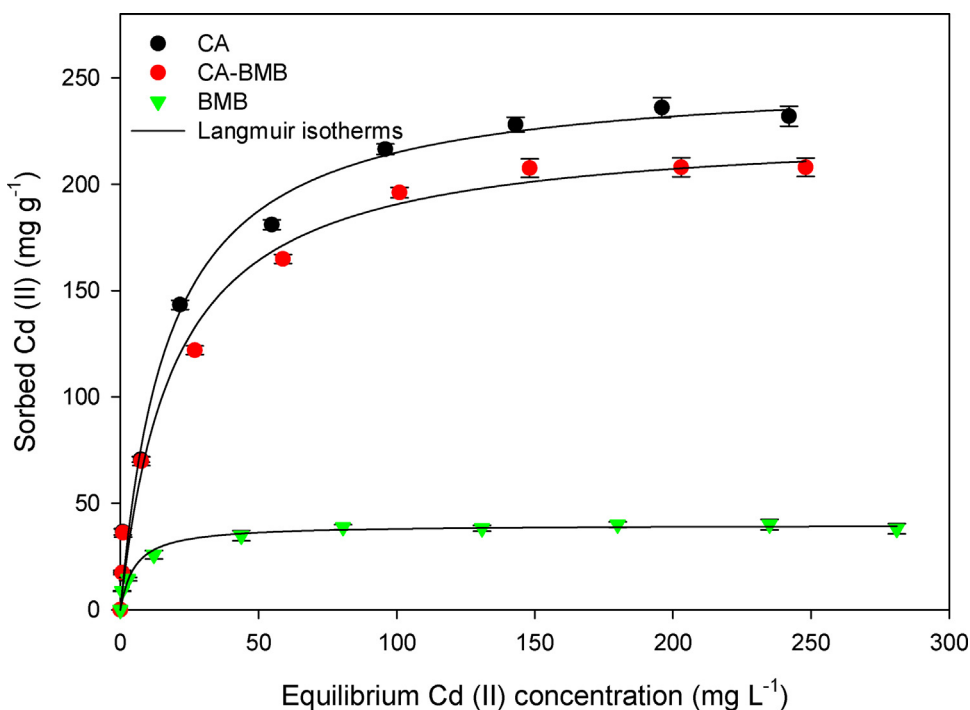

Fig. 5. Equilibrium sorption isotherm for Cd(II) onto CA, BMB and CA-BMB (adsorbent dose 250 mg L^{-1}, contact time 24 h, temperature 25 °C, Cd(II) solution 40 mL, and pH 5.0). Data modeled using Langmuir model (solid lines). Error bars represent standard error of triplicate samples (n = 3). Symbols may cover error bars.

Table 3
A comparison of the adsorption capacities of the other adsorbents for Cd(II).

Adsorbent	Q_m (mg g^{-1})	Ref.
Prepared alginate bead	234.9	[42]
Activated carbon	93.4	[43]
Modified electronic	236	[5]
Vermiculite	71.0	[44]
Modified biochar	28.1	[45]
Hickory modified biochar	53.6	[46]
Dairy manure biochar	51.4	[10]
MWCNTs	10.86	[47]
Activated sludge	204.1	[48]
Modified maize straw	196.1	[49]
Ca-alginate	36.6	[50]
Ball-milled biochar	40.0	This study
Ca-algnate-BMB	227.1	This study
Ca-alginate bead	251.8	This study

the maximum Cd(II) adsorption capacity for BMB was 40.0 mg g^{-1}, which is close to that of activated carbon from bagasse [40]. The maximum Cd(II) adsorption capacity for CA and CA-BMB is 251.8 mg g^{-1} and 227.1 mg g^{-1}, respectively, much higher than that of BMB. The highest Cd(II) sorption capacity of CA among the three sorbents may indicate that CA contains more surface acidic oxygen-containing functional groups than BMB and CA-BMB, and thus more adsorption sites for Cd(II) exchange with calcium (II) ions. These acidic oxygen-containing functional groups are beneficial to raise the cadmium binding by bridging or bidentate complex formation with the carboxyl groups of the alginate [41]. Compared with many other adsorbents, including other Ca-alginate composites, the CA-BMB in this work possessed high Cd(II) adsorption capacity (Table 3).

Also note that the higher adsorption capacity of CA-BMB than BMB could be partly due to the high adsorption capacity of CA. However, considering the mixing ratio of CA to BMB, the enhanced adsorption capacity of CA-BMB over BMB cannot be simply due to the high adsorption capacity of CA. The synergetic effect between CA and BMB in enhancing Cd(II) adsorption (Fig. 5) can be understood in a context that CA interacted with BMB in exposing active sorption sites for both BMB and CA during the impregnation of nanosized BMB in CA. Furthermore, the price of biochar is much lower than alginate, it would thus be more cost-effective to use CA-BMB beads instead CA beads in large scale applications.

Conclusions

This study confirmed that entrapment of ball-milled biochar in Ca-alginate beads provided a novel and effective adsorbent for removal of Cd(II) in aqueous solution. The optimum pH for Cd(II) adsorption was 5 for ball-milled biochar entrapped in Ca-alginate beads. The maximum Cd(II) adsorption capacity estimated with Langmuir isotherm modeling was 227.1 mg g^{-1} for ball-milled biochar entrapped in Ca-alginate beads, much larger than that of ball-milled biochar alone (40.0 mg g^{-1}). The ball-milled biochar entrapped in Ca-alginate can be also applied in fixed-bed operations, which provides additional advantages.

Acknowledgements

References

[1] D. Ghosh, R. Saha, A. Ghosh, R. Nandi, B. Saha, Desalin. Water Treat. 53 (2015) 413.
[2] Q. Zhao, Y. Wang, Y. Cao, A. Chen, M. Ren, Y. Ge, Z. Yu, S. Wan, A. Hu, Q. Bo, L. Ruan, H. Chen, S. Qin, W. Chen, C. Hu, F. Tao, D. Xu, J. Xu, L. Wen, L. Li, Sci. Total Environ. 470–471 (2014) 340.
[3] Z. Li, Z. Ma, T.J. van der Kuijp, Z. Yuan, L. Huang, Sci. Total Environ. 468–469 (2014) 843.
[4] S.E. Bailey, T.J. Olin, R.M. Bricka, D.D. Adrian, Water Res. 33 (1999) 2469.
[5] M. Xu, P. Hadi, G. Chen, G. McKay, J. Hazard. Mater. 273 (2014) 118.
[6] X. Luo, L. Zhang, J. Hazard. Mater. 171 (2009) 340.
[7] M. Ahmad, A.U. Rajapaksha, J.E. Lim, M. Zhang, N. Bolan, D. Mohan, M. Vithanage, S.S. Lee, Y.S. Ok, Chemosphere 99 (2014) 19.
[8] D. Mohan, A. Sarswat, Y.S. Ok, C.U. Pittman Jr., Bioresour. Technol. 160 (2014) 191.
[9] M.I. Inyang, B. Gao, Y. Yao, Y. Xue, A. Zimmerman, A. Mosa, P. Pull-ammanappallil, Y.S. Ok, X. Cao, Crit. Rev. Environ. Sci. Technol. 46 (2016) 406.
[10] X. Xu, X. Cao, L. Zhao, H. Wang, H. Yu, B. Gao, Environ. Sci. Pollut. Res. 20 (2013) 358.
[11] F.Y. Wang, H. Wang, J.W. Ma, J. Hazard. Mater. 177 (2010) 300.
[12] H. Wu, C. Lai, G. Zeng, J. Liang, J. Chen, J. Xu, J. Dai, X. Li, J. Liu, M. Chen, L. Lu, L. Hu, J. Wan, Crit. Rev. Biotechnol. 37 (2017) 754.
[13] G. Zeng, H. Wu, J. Liang, S. Guo, L. Huang, P. Xu, Y. Liu, Y. Yuan, X. He, Y. He, RSC Adv. 5 (2015) 34541.
[14] Y. Sun, B. Gao, Y. Yao, J. Fang, M. Zhang, Y. Zhou, H. Chen, L. Yang, Chem. Eng. J. 240 (2014) 574.
[15] Y. Xue, B. Gao, Y. Yao, M. Inyang, M. Zhang, A.R. Zimmerman, K.S. Ro, Chem. Eng. J. 200 (2012) 673.
[16] A.U. Rajapaksha, S.S. Chen, D.C. Tsang, M. Zhang, M. Vithanage, S. Mandal, B. Gao, N.S. Bolan, Y.S. Ok, Chemosphere 148 (2016) 276.
[17] Y. Zhou, B. Gao, A.R. Zimmerman, J. Fang, Y. Sun, X. Cao, Chem. Eng. J. 231 (2013) 512.
[18] Y. Zhou, B. Gao, A.R. Zimmerman, H. Chen, M. Zhang, X. Cao, Bioresour. Technol. 152 (2014) 538.
[19] S. Wang, B. Gao, A.R. Zimmerman, Y. Li, L. Ma, W.G. Harris, K.W. Migliaccio, Bioresour. Technol. 175 (2015) 391.
[20] M. Zhang, B. Gao, S. Varnoosfaderani, A. Hebard, Y. Yao, M. Inyang, Bioresour. Technol. 130 (2013) 457.
[21] Y. Zhou, X. Liu, Y. Xiang, P. Wang, J. Zhang, F. Zhang, J. Wei, L. Luo, M. Lei, L. Tang, Bioresour. Technol. 245 (2017) 266.
[22] Y. Zhou, X. Liu, L. Tang, F. Zhang, G. Zeng, X. Peng, L. Luo, Y. Deng, Y. Pang, J. Zhang, J. Hazard. Mater. 333 (2017) 80.
[23] X. Peng, X. Liu, Y. Zhou, B. Peng, L. Tang, L. Luo, B. Yao, Y. Deng, J. Tang, G. Zeng, RSC Adv. (2017) 8755.
[24] S. Ye, G. Zeng, H. Wu, C. Zhang, J. Dai, J. Liang, J. Yu, X. Ren, H. Yi, M. Cheng, C. Zhang, Crit. Rev. Biotechnol. 37 (2017) 1062.
[25] H. Lyu, B. Gao, F. He, A. Zimmerman, C. Ding, H. Huang, J. Tang, J. Crittenden, Chem. Eng. J. 335 (2018) 110.
[26] H. Lyu, B. Gao, F. He, A. Zimmerman, C. Ding, H. Huang, J. Tang, Environ. Pollut. 233 (2018) 54.
[27] S.C. Peterson, M.A. Jackson, S. Kim, D.E. Palmquist, Powder Technol. 228 (2012) 115.
[28] H. Lyu, B. Gao, F. He, C. Ding, J. Tang, J.C. Crittenden, ACS Sustain. Chem. Eng. 5 (2017) 9568.
[29] D. Wang, W. Zhang, X. Hao, D. Zhou, Environ. Sci. Technol. 47 (2013) 821.
[30] W. Zhang, J. Niu, V.L. Morales, X. Chen, A.G. Hay, J. Lehmann, T.S. Steenhuis, Ecohydrology 3 (2010) 497.
[31] R.S. Kookana, Soil Res. 48 (2010) 627.
[32] M. Chen, D. Wang, F. Yang, X. Xu, N. Xu, X. Cao, Environ. Pollut. 230 (2017) 540.
[33] K.Y. Lee, D.J. Mooney, Prog. Polym. Sci. 37 (2012) 106.
[34] X.-H. Do, B.-K. Lee, J. Environ. Manage. 131 (2013) 375.
[35] K.-W. Jung, T.-U. Jeong, H.-J. Kang, K.-H. Ahn, Bioresour. Technol. 211 (2016) 108.
[36] H. Roh, M.-R. Yu, K. Yakkala, J.R. Koduru, J.-K. Yang, Y.-Y. Chang, J. Ind. Eng. Chem. 26 (2015) 226.
[37] D. Kołodyńska, R. Wnętrzak, J.J. Leahy, M.H.B. Hayes, W. Kwapiński, Z. Hubicki, Chem. Eng. J. 197 (2012) 295.
[38] V.C. Taty-Costodes, H. Fauduet, C. Porte, A. Delacroix, J. Hazard. Mater. 105 (2003) 121.
[39] Y.-H. Li, Z. Di, J. Ding, D. Wu, Z. Luan, Y. Zhu, Water Res. 39 (2005) 605.
[40] D. Mohan, K.P. Singh, Water Res. 36 (2002) 2304.
[41] E. Fourest, B. Volesky, Environ. Sci. Technol. 30 (1996) 277.
[42] S. Papageorgiou, E. Kouvelos, F. Katsaros, Desalination 224 (2008) 293.
[43] K. Kadirvelu, C. Namasivayam, Adv. Environ. Res. 7 (2003) 471.
[44] E. Padilla-Ortega, R. Leyva-Ramos, J. Mendoza-Barron, Appl. Clay Sci. 88–89 (2014) 10.

[45] H. Wang, B. Gao, S. Wang, J. Fang, Y. Xue, K. Yang, Bioresour. Technol. 197 (2015) 356.

[46] Z. Ding, X. Hu, Y. Wan, S. Wang, B. Gao, J. Ind. Eng. Chem. 33 (2016) 239.

[47] Y.-H. Li, J. Ding, Z. Luan, Z. Di, Y. Zhu, C. Xu, D. Wu, B. Wei, Carbon 41 (2003) 2787.

[48] R.D.C. Soltani, A.J. Jafari, G.S. Khorramabadi, Am. J. Environ. Sci. 5 (2009) 41.

[49] H. Guo, S. Zhang, Z. Kou, S. Zhai, W. Ma, Y. Yang, Carbohydr. Polym. 115 (2015) 177.

[50] Y. Kaçar, Ç. Arpa, S. Tan, A. Denizli, Ö. Genç, M.Y. Arıca, Process Biochem. 37 (2002) 601.